The Journal of Immunology

KIR/HLA Interactions Negatively Affect Rituximab- but Not GA101 (Obinutuzumab)-Induced Antibody-Dependent Cellular Cytotoxicity

Grzegorz Terszowski, Christian Klein and Martin Stern

J Immunol 2014; 192:5618-5624; Prepublished online 2 May 2014;
doi: 10.4049/jimmunol.1400288
http://www.jimmunol.org/content/192/12/5618

The Journal of Immunology is published twice each month by
The American Association of Immunologists, Inc.,
9650 Rockville Pike, Bethesda, MD 20814-3994.

Print ISSN: 0022-1767 Online ISSN: 1550-6606.

KIR/HLA Interactions Negatively Affect Rituximab- but Not GA101 (Obinutuzumab)-Induced Antibody-Dependent Cellular Cytotoxicity

Grzegorz Terszowski,* Christian Klein,† and Martin Stern*

Ab-dependent cellular cytotoxicity (ADCC) mediated by NK cells is regulated by inhibitory killer cell Ig–like receptors (KIRs), which interact with target cell HLA class I. We analyzed how KIR/HLA interactions influence ADCC induced by rituximab and by GA101, a novel type II CD20 Ab glycoengineered for increased FcgRIII binding and ADCC capacity. We found that KIR/HLA interactions strongly and selectively inhibit rituximab-induced in vitro ADCC toward target cells expressing cognate HLA KIR ligands. NK cells of donors carrying all three ligands to inhibitory KIR showed weak activation and target cell depletion capacity when incubated with rituximab and KIR-ligand matched target B cells. In contrast, NK cells from individuals missing one or more KIR ligands activated more strongly and depleted KIR ligand–matched target B cells more efficiently in the presence of rituximab. NK cells expressing a KIR for which the ligand was absent were the main effectors of ADCC in these donors. Notably, the influence of KIR/HLA interactions on NK cell activation was synergistic with the effect of the V158F FCGR3A single nucleotide polymorphism. In contrast, GA101 induced activation of NK cells irrespective of inhibitory KIR expression, and efficiency of target cell depletion was not negatively affected by KIR/HLA interactions. These data show that modification of the Fc fragment to enhance ADCC can be an effective strategy to augment the efficacy of therapeutic mAbs by recruiting NK cells irrespective of their inhibitory KIR expression. ***The Journal of Immunology*****, 2014, 192: 5618–5624.**

Monoclonal Abs have revolutionized the treatment of many cancers (1). In particular, Abs against CD20 are successfully applied in the therapy of B cell lymphomas (2). Introduced in 1997, the chimeric Ab rituximab is the standard of care in the treatment of these malignancies and remains the reference molecule against which novel Abs are compared. The success of rituximab is based on its efficacy to induce remission in both low-grade and high-grade lymphomas, either as a single agent and/or in combination with cytotoxic chemotherapy (3). However, significant portions of patients do not respond to, or relapse after, rituximab treatment, which has led to the development of novel CD20 Abs. These molecules differ from rituximab in the epitope of CD20 they bind, or are otherwise modified to improve effector function (4). Classically, CD20 Abs are thought to deplete target cells by inducing direct cell death, by activating the complement system (complement-dependent cytotoxicity), and by recruiting effector cells for Ab-dependent cellular cytotoxicity (ADCC) (2).

One such Ab with improved effector function is GA101 (obinutuzumab), a novel glycoengineered type II CD20 mAb that differs in important aspects from rituximab: 1) as a type II CD20 Ab, it does not relocalize CD20 into lipid rafts upon binding, resulting in decreased complement-dependent cytotoxicity, but it increases direct cell death; and 2) the Fc portion was glycoengineered to reduce fucosylation, resulting in increased affinity to the human Fc receptor FCGR3A (CD16) (5). The rationale to modify the Fc portion of the Ab derives from data showing that the affinity between mAbs and FCGR3A is important for clinical efficacy. This is demonstrated by a single nucleotide polymorphism (SNP; V158F) in the FCGR3A gene, which influences IgG1-Fc binding to FCGR3A. Several clinical studies demonstrated that patients carrying two high-affinity (V) alleles respond better to rituximab and other mAbs than do patients carrying one or two low-affinity (F) alleles (6–8), although some studies in lymphoma patients failed to replicate this association (9, 10). In vitro, engagement of target cells by mAbs can result in ADCC and target cell lysis. The association of FCGR3A polymorphisms with treatment efficacy suggests that this mechanism is also important in vivo.

The major cell population performing ADCC are NK cells, of which in the peripheral blood pool ~90% express FCGR3A (11). NK cells coexpress a wide array of surface receptors with activating or inhibitory function, which potentially influence that capacity for ADCC. In particular, NK cells carry inhibitory killer cell Ig–like receptors (KIRs), which interact with public epitopes on HLA class I Ags (KIR2DL1 with HLA-C Ags sharing the C2 specificity; KIR2DL3 with HLA-C Ags sharing the C1 specificity; and KIR3DL1 with HLA-A and -B Ags sharing the Bw4 specificity) (12). The KIR/HLA interaction has a dual function: during NK cell development in the bone marrow, recognition of HLA by inhibitory KIRs leads to terminal differentiation and acquisition of full effector function in a poorly understood process termed "licensing." A functional advantage of licensed over unlicensed NK

*Department of Biomedicine, University Hospital Basel, CH-4031 Basel, Switzerland; and †Pharma Research and Early Development, Roche Glycart AG, CH-8952 Schlieren, Switzerland

Received for publication January 31, 2014. Accepted for publication April 2, 2014.

This work was supported Swiss National Science Foundation Grant PPOOP3 128461/1 (to M.S.) and by grants from Roche/University Hospital Basel Translational Medicine Hub (to M.S. and G.T.).

G.T. performed experiments and G.T., C.K., and M.S. designed the research, analyzed data, and wrote the paper.

Address correspondence and reprint requests to Prof. Martin Stern, Department of Biomedicine, University Hospital Basel, Hebelstrasse 20, CH-4031 Basel, Switzerland. E-mail: martin.stern@usb.ch

The online version of this article contains supplemental material.

Abbreviations used in this article: ADCC, Ab-dependent cellular cytotoxicity; CLL, chronic lymphocytic leukemia; KIR, killer cell Ig–like receptor; MFI, mean fluorescence intensity; SNP, single nucleotide polymorphism.

www.jimmunol.org/cgi/doi/10.4049/jimmunol.1400288

cells was observed using different stimulation methods such as challenge with HLA-deficient target cells, Ab crosslinking, and ADCC (13). The molecular mechanism responsible for increased functionality of licensed cells has so far not been elucidated. Once released into the blood, inhibitory KIRs again interact with tissue HLA, providing one of the main mechanisms of NK cell tolerance (12).

Previous studies have shown that licensing status affects the capacity for activation through FCGR3A (13), and that inhibitory signals derived from the KIR/HLA interaction may negatively affect NK cell–mediated ADCC (14, 15). We therefore asked how KIR/HLA interactions influence ADCC, and whether differences exist between conventional and glycoengineered Abs.

Materials and Methods

Samples and cell lines

Healthy donor buffy coats were collected after written informed consent from all study participants. PBMCs were purified by centrifugation on density gradient using Lymphoprep (Axis-Shield, Oslo, Norway). After isolation, PBMCs were aliquoted and cryopreserved in 10% DMSO, 50% heat-inactivated FBS (Sigma-Aldrich, St. Louis, MO), and 40% DMEM medium for later use. Primary chronic lymphocytic leukemia (CLL) cells were collected from peripheral blood of untreated patients under an Ethical Committee–approved protocol, purified by Lymphoprep separation, and cryopreserved in liquid nitrogen until use.

The following cell lines were used as targets for functional assays: the HLA-deficient EBV-transformed B lymphoblastoid cell line 721.221; 721.221 cells transfected with the HLA-C2 group epitope Cw*0401; 721.221 cells transfected with the HLA-Bw4 group epitope B*5801; the lymphoblastoid B cell lines SPL (HLA-A*3101, B*1501, C* 0102 [$C1^+C2^-Bw4^-$]); FH7 (HLA-A*0206/3002, B*3908/1801, C*0702/0501 [$C1^+C2^+Bw4^-$]); WT47 (HLA-A*3201, B*4402, C*0501 [$C1^-C2^+Bw4^+$]); and BatJ (HLA-A*0201/3101, B*4001/4402, C*0501 [$C1^+C2^+Bw4^+$]). All cell lines were grown in RPMI 1640 medium (Life Technologies, Carlsbad, CA) supplemented with 10% (v/v) heat-inactivated human AB serum (Basel University Hospital Blood Bank), penicillin (100 U/ml), and streptomycin (10 μg/ml) (Life Technologies).

KIR, KIR ligand, and FCGR3A genotyping

Genomic DNA of PBMCs was isolated from 200 μl whole blood using a commercial kit (QIAamp DNA kit from Qiagen). The presence of inhibitory KIR ligands (HLA-C1, HLA-C2, and HLA-Bw4) was assessed using published protocols (16, 17). The KIR genotype was analyzed with Luminex technology using the KIR SSO genotyping test (One Lambda, Canoga Park, CA). Donors positive for KIR2DL2 (an allele of KIR2DL3 that interacts with both C1 and C2 epitopes) were excluded from the analysis. The FCGR3A V158F polymorphism was typed by allele-specific PCR according to a published protocol (18).

mAbs and flow cytometry

The following mAbs were used: anti-CD3 allophycocyanin-eFluor 780 (clone SK7, eBioscience, San Diego, CA), anti-CD14 allophycocyanin-eFluor 780 (clone 61D3, eBioscience), anti-CD19 allophycocyanin-eFluor 780 (clone HIB19, eBioscience), anti-CD56 PE-C7 (clone HCD56, BioLegend, San Diego, CA), anti-CD107a PE (clone H4A3, BD Biosciences), anti-CD107a BD Horizon V450 (clone H4A3, BD Biosciences), anti-CD158a (2DL1) FITC (clone 143211, R&D Systems), anti-CD158b (2DL2/DL3) PerCP (clone DX27, Miltenyi Biotec, Bergisch Gladbach, Germany), anti-CD158e (3DL1) Brilliant Violet 421 (clone DX9, BioLegend), and anti-CD159a (NKG2A) PE (clone Z199, Beckman Coulter, Marseille, France). Rituximab was purchased from Roche (Basel, Switzerland). GA101 and its non-glycoengineered parent molecule (wt-GA101) were provided by Roche Glycart (Schlieren, Switzerland).

Human FcR blocking reagent (Miltenyi Biotec) was used to improve the specificity of staining. Samples were acquired using a Dako CyAn ADP nine-color flow cytometer (Beckman Coulter, Pasadena, CA). Results were analyzed using FlowJo version 9.6 software (Tree Star, Ashland, OR).

The strategy to define single KIR2DL1-, KIR2DL3-, or KIR3DL1-expressing NK cells is illustrated in Supplemental Fig. 1. NK cells were defined in the gate of lymphocytes as $CD3^-CD14^-CD19^-CD56^+$ cells (all target cells were gated out by inclusion of CD19 in the panel). Next, populations of interest were separated after sequential gating based on expression of NKG2A, KIR2DL1, KIR2DL3, and KIR3DL1. In summary, single KIR2DL1 NK cells (single 2DL1 panel D) were defined as $KIR2DL1^+KIR2DL3^-KIR3DL1^-NKG2A^-$ (panels A, B, and D); single KIR3DL1 as $KIR2DL1^-KIR2DL3^-KIR3DL1^+NKG2A^-$ (panels A, B, and E), and single KIR2DL3 NK cells as $KIR2DL1^-KIR2DL3^+KIR3DL1^-NKG2A^-$ (panels A, C, and F). The level of degranulation (CD107a) was used as a marker of NK cell activation (19). The CD107a background level was determined after incubation of effector cells without target cells (panels G, H, and I). Experiments using isotype-matched control Abs were used to set gates for flow cytometric analyses.

Functional assays

For functional assays, PBMCs were thawed and cultured overnight in DMEM supplemented with 10% (v/v) heat-inactivated FBS, penicillin (100 U/ml), and streptomycin (10 μg/ml). The following day, PBMCs were mixed with target cells at an E:T ratio of 10:1 in the presence of CD107a Ab in U-bottom 96-well plates. Fifty percent heat-inactivated human AB serum was added as a source of polyclonal IgG. Anti-CD20 Abs were added to a final concentration 0.1, 1, or 10 μg/ml in experiments using as targets the lymphoblastoid B cell lines. Primary CLL cells, which express CD20 weakly (20), were treated with the Abs at a final concentration of 5 μg/ml to allow NK cell activation with rituximab at comparable levels as cell lines treated at 0.1 μg/ml. Cells were incubated for 6 h. Brefeldin A (BD Biosciences) was added after 1 h. After incubation, cells were stained and analyzed by flow cytometry.

To estimate the rate of killing by NK cells, we used a mixed target cell depletion/degranulation assay. Briefly, NK cells were isolated using a human NK cell isolation kit (Miltenyi Biotec) and incubated with target cells labeled with eFluor 670 dye (eBioscience) at an E:T ratio of 2:1. Brefeldin A was added after 5 h. After 6 h of incubation, cells were stained and analyzed by flow cytometry. The percentage of killing was calculated according to the measured loss of eFluor 670^+ cells compared with controls containing target cells alone.

Statistical analysis

Degranulation of NK cell subsets and target cell depletion were compared by paired or unpaired *t* tests or by ANOVA, respectively. The frequency of licensed NK cells was correlated to target cell depletion by linear regression.

Results

Licensing status affects capacity for ADCC

To address how licensing status affects the capacity for ADCC, we assessed degranulation in NK cells after coincubation with the HLA-deficient target cell 721.221 in the absence of a mAb ("missing self" recognition) and in the presence of rituximab, GA101, and the non-glycoengineered parent molecule wt-GA101. In agreement with previous studies, we found that licensing affected the missing self reaction (degranulation in licensed cells 35 ± 4% versus 19 ± 3% of unlicensed cells, $p < 0.01$), as well as rituximab-mediated ADCC (degranulation in licensed cells 46 ± 4% versus 29 ± 5% in unlicensed cells, $p = 0.01$; Fig. 1A) (13). Notably, both wt-GA101 and GA101 were more efficient than rituximab in activating NK cells. Whereas a trend for a difference between licensed and unlicensed NK cells was still seen in wt-GA101–treated 721.221 cells (degranulation in licensed cells 60 ± 5% versus 48 ± 5% in unlicensed cells, $p = 0.09$), no significant difference was detected in the number of NK cells responding to GA101-treated 721.221 cells (75 ± 4% versus 67 ± 4%, $p = 0.23$, Fig. 1A). Using paired analysis, we compared activation of unlicensed NK cells to that of licensed NK cells from the same donor, and we found that the frequency of degranulating NK cells in unlicensed cells was 54, 18, and 9% lower after incubation with 721.221 cells and rituximab, wt-GA101, and GA101, respectively ($p < 0.01$ for comparison between the three Abs).

KIR/HLA interaction blocks ADCC

To analyze how the presence of a cognate HLA class I KIR ligand affects activation of KIR-expressing NK cells, we used as targets

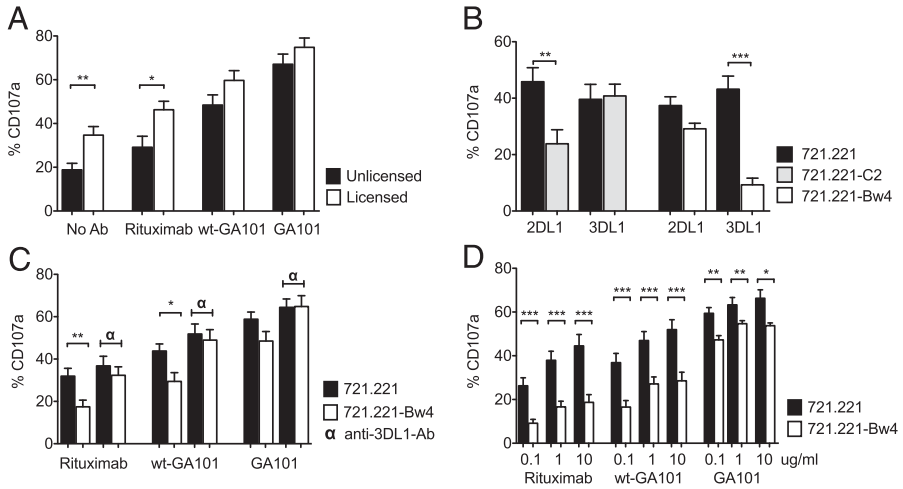

FIGURE 1. KIR/HLA interactions influence ADCC. PBMCs were incubated with target cells in the absence or presence of anti-CD20 Abs. After incubation, cells were stained and analyzed using flow cytometry. NK cell subpopulations were electronically gated and the percentage of $CD107a^+$ cells was used to determine the degranulation/activation level (Supplemental Fig. 1). Bars represent the mean (±SE) percentage of $CD107a^+$ cells among the investigated subpopulation. (**A**) Licensing status positively affects ADCC. PBMCs from individuals (n = 12) expressing different configurations of HLA ligands and all three relevant KIR receptors (KIR2DL1, KIR2DL3, and KIR3DL1) were incubated with HLA-deficient 721.221 target cells with or without CD20 Abs (0.1 μg/ml). The percentage of degranulation was analyzed in single KIR^+NKGA^- NK cells, grouped to unlicensed and licensed populations according to the presence of HLA ligands in individuals. (**B**) KIR/HLA interactions inhibit ADCC. PBMCs from $HLA\text{-}C2^+$ and $Bw4^+$ individuals (n = 14) expressing KIR2DL1 and KIR3DL1 were incubated with HLA^- (721.221) target cells or cells that either expressed a ligand from the C2 group (721.221-Cw*0401) or a ligand from the Bw4 group (721.221-B*5801) in the presence of rituximab (0.1 μg/ml). The percentage of degranulation was compared between single $KIR2DL1^+$ and single $KIR3DL1^+$ NK cells in response to target cells. (**C**) Influence of the KIR3DL1/HLA-Bw4 interaction on ADCC induced with rituximab, wt-GA101, and GA101. PBMCs from $HLA\text{-}Bw4^+$, $KIR3DL1^+$ individuals (n = 8) were incubated with either 721.221 or 721.221-B*5801 (Bw4) target cells treated with CD20 Abs (0.1 μg/ml). To block the inhibitory interaction between KIR3DL1 and its ligand HLA-Bw4, the anti-CD158e (3DL1) Ab (clone DX9) was added at a concentration of 10 μg/ml to the effector cells before incubation with targets. The percentage of $CD107a^+$ expression within single $KIR3DL1^+$ NK cells was compared. (**D**) Increased concentration of CD20 Ab does not abolish the inhibitory effect of the interaction between KIR3DL1 and its ligand. Target cells were treated with escalating doses of CD20 Abs (0.1, 1, and 10 μg/ml) and incubated with PBMCs from $HLA\text{-}Bw4^+$, $KIR3DL1^+$ individuals (n = 8). The percentage of $CD107a^+$ expression within single $KIR3DL1^+$ NK cells was compared. $*p \leq 0.05$, $**p \leq 0.01$, $***p \leq 0.001$.

721.221 cells transfected with single HLA Ags (either HLA-Cw*0401 [721.221-C2] as a ligand to KIR2DL1, or HLA-B*5801 [721.221-Bw4] as a ligand to KIR3DL1). An overview of KIR ligand status of cell lines used is presented in Table I. Expression of the cognate KIR ligand significantly and specifically inhibited activation of NK cells expressing the corresponding inhibitory KIR receptors in ADCC experiments using rituximab (Fig. 1B).

We next compared the effect of the KIR3DL1/HLA-Bw4 interaction on ADCC in cells treated with rituximab, wt-GA101, and GA101. We detected significant inhibition of degranulation by KIR/HLA interactions when target cells were treated with rituximab (CD107a expression 17 ± 3% against 721.221-Bw4 cells, compared with 32 ± 4% against 721.221 cells, $p < 0.01$). Treatment of target cells with wt-GA101 increased degranulation against both target cells with a significant inhibitory effect of HLA remaining (29 ± 4% against 721.221-Bw4 versus 44 ± 3% against 721.221, $p = 0.02$). Of note, GA101 was even more effective in activating NK cells, and differences between target cells no longer reached the level of statistical significance (49 ± 4% in 721.221-Bw4 versus 59 ± 3% in 721.221, $p = 0.08$). Blocking the KIR/HLA interaction using an Ab directed against KIR3DL1 rescued NK cell activation up to the level of HLA-deficient target cells with all CD20 Abs including GA101, showing that activation of NK cells by GA101 is not completely refractory to inhibitory KIR signaling (Fig. 1C). On average, the presence of an inhibitory KIR ligand decreased NK cell activation by 46% in samples treated with rituximab, by 34% in samples treated with wt-GA101, and by 19% in samples treated with GA101 (overall $p < 0.01$). In contrast to blocking with anti-KIR Abs, escalation of the dose of CD20 bodies (from 0.1 to 1 and 10 μg/ml) increased total NK cell activation (particularly for rituximab and wt-GA101), but did not abolish the negative effect of the KIR3DL1/HLA-Bw4 interaction (Fig. 1D).

Unlicensed NK cells are the primary ADCC effector cells in individuals lacking a KIR ligand

Because the KIR/HLA interaction has both positive and negative effects on the capacity to mediate ADCC (licensing during NK cell education versus inhibitory signaling during target cell encounter), we next addressed which of these mechanisms was more relevant during ADCC. To this end, we analyzed rituximab-induced NK cell activation in donors expressing the KIR ligands C2 and Bw4, but lacking a C1 ligand (recognized by KIR2DL3) after coincubation with a target B cell line expressing the same ligands (WT47). These

Table I. KIR ligand status of cell lines used

	721.221	721.221-C2	721.221-Bw4	SPL	FHL	BatJ
C1 (KIR2DL3-L)				X	X	X
C2 (KIR2DL1-L)		X			X	X
Bw4 (KIR3DL1-L)			X			X

experiments showed that degranulation was strongest (55 ± 3%) in KIR2DL3$^+$ NK cells unable to engage target cell HLA. In contrast, degranulation was low in NK cells expressing KIR2DL1 (12 ± 2%) or KIR3DL1 (10 ± 2%, Fig. 2A). Control experiments using NK cells from donors carrying all three KIR ligands and the HLA-deficient target cell 721.221 showed similar activation of all KIR$^+$ NK cell subsets, excluding intrinsic differences in reactivity between subsets expressing different inhibitory KIR receptors (data not shown). Collectively, these data demonstrate that the inhibitory effect during target cell encounter dominates over the activating effect of NK cell licensing, leading to unlicensed NK cells being the strongest effectors of ADCC with rituximab.

Activation by GA101 compensates for inhibitory KIR/HLA interactions

Because efficient ADCC with rituximab required the absence of a KIR ligand, we next asked whether glycoengineered Abs through their higher affinity for FCGR3A are able to overcome the inhibitory signal derived from the KIR/HLA interaction. We therefore assessed NK cell degranulation in individuals carrying all three KIR ligands in ADCC experiments using KIR ligand–matched target B cells, comparing activation of NK cells carrying no, one, two, or all three inhibitory KIR receptors. In experiments using rituximab, NK cell activation decreased with growing number of inhibitory KIR expressed. A similar pattern was seen for wt-GA101 and GA101, but at higher levels of activation for all subsets analyzed (Fig. 2B). Interestingly, on a quantitative level, rituximab-induced activation of NK cells was comparable to GA101-induced activation of NK cells expressing two additional KIRs (rituximab with no KIR, 31 ± 3%; GA101 with two KIRs, 29 ± 2%; rituximab with one KIR, 21 ± 2%; and GA101 with three KIRs, 20 ± 3%; Fig. 2B).

The capacity of GA101 to compensate for inhibitory KIR/HLA interactions was further tested in experiments involving NK cells and KIR ligand–matched B cell targets. Activation by ADCC against target cells lacking two (SPL) or one (FH7) KIR ligands was essentially restricted to unlicensed NK cells devoid of KIRs able to recognize ligands on target cells in experiments using rituximab. In contrast, GA101 induced similar activation of all NK cell subsets, irrespective of inhibitory KIR expression (Fig. 2C, 2D). Similarly, using the BatJ cell line expressing all KIR ligands, degranulation of KIR$^+$ NK cell subsets was low with rituximab (between 8 and 11% for the three KIR subsets), increasing to 15–20% for wt-GA101, and to 39–44% for GA101 (Fig. 2E).

GA101 induces stronger degranulation on a single cell basis

Having established that, compared with rituximab, GA101 is able to recruit more (licensed, KIR$^+$) NK cells to participate in ADCC, we wondered whether the strength of degranulation on a single cell level was also different between these Abs. We therefore compared the mean fluorescence intensity (MFI) of CD107a expression on NK cells after rituximab-, wt-GA101–, or GA101-induced ADCC. GA101 not only recruited more NK cells for ADCC (representative sample experiment in Fig. 2C, 75 versus 30%), but also increased mean CD107a expression in responding cells (MFI 320 versus 210 in rituximab-induced ADCC, Fig. 3A). On average, CD107a MFI increased from 214 ± 14 (rituximab) to 267 ± 19 (wt-GA101) to 335 ± 22 (GA101, $p < 0.01$, Fig. 3B), demonstrating that in addition to recruiting more NK cells, GA101 was more efficient in activating NK cells at the single cell level.

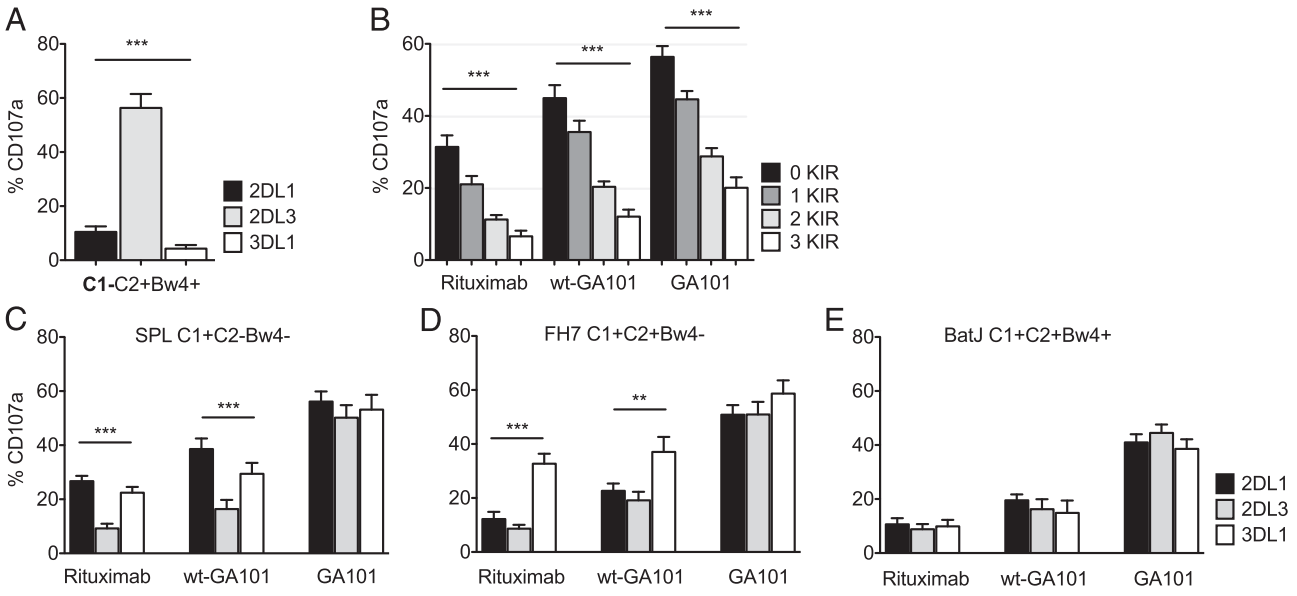

FIGURE 2. GA101 compensates for inhibition by KIR/HLA interactions of licensed NK cells activation. (**A**) Inhibitory KIR/HLA interactions abolish the positive effect of NK cell licensing. PBMCs from HLA-C1$^-$, C2$^+$, and Bw4$^+$ individuals (n = 10) expressing all three inhibitory KIR receptors were incubated with a KIR ligand–matched lymphoblastoid B cell line (WT47 HLA-A*3201, B*4402, C*0501 [C1$^-$C2$^+$Bw4$^+$]). The degranulation level was compared between NKG2A$^-$ NK cell subpopulations carrying single KIR2DL1, KIR2DL3, or KIR3DL1. (**B**) The inhibitory KIR signal is compensated by GA101. The ability to induce NK cell activation with rituximab, wt-GA101, and GA101 in the presence of increasing levels of inhibition was assessed by comparing the degranulation in NKG2A$^-$ NK cell subpopulations expressing no, one, two, or three inhibitory KIR receptors after exposure to target cells treated with CD20 Abs (0.1 μg/ml). To this end, PBMCs from individuals (n = 11) carrying all three inhibitory receptors and their ligands were incubated with a cell line expressing all three relevant HLA KIR ligands (BatJ HLA-A*0201/3101, B*4001/4402, and C*0501 [C1$^+$C2$^+$Bw4$^+$]). (**C**–**E**) ADCC induced by rituximab but not GA101 is restricted to unlicensed NK cells. The percentage of CD107a$^+$ cells among single KIR$^+$ NK cell subpopulations was measured after incubation of PBMCs from individuals (n = 12/genotype) carrying one, two, or three inhibitory KIR ligands with B cell lines matched for KIR ligand (SPL HLA-A*3101, B*1501, C* 0102 [C1$^+$C2$^-$Bw4$^-$] (C); FH7 HLA-A*0206/3002, B*3908/1801, C*0702/0501 [C1$^+$C2$^+$Bw4$^-$] (D); and BatJ HLA-A*0201/3101, B*4001/4402, and C*0501 [C1$^+$C2$^+$Bw4$^+$] (E) treated with CD20 Abs (0.1 μg/ml). $^{**}p \leq 0.01$, $^{***}p \leq 0.001$.

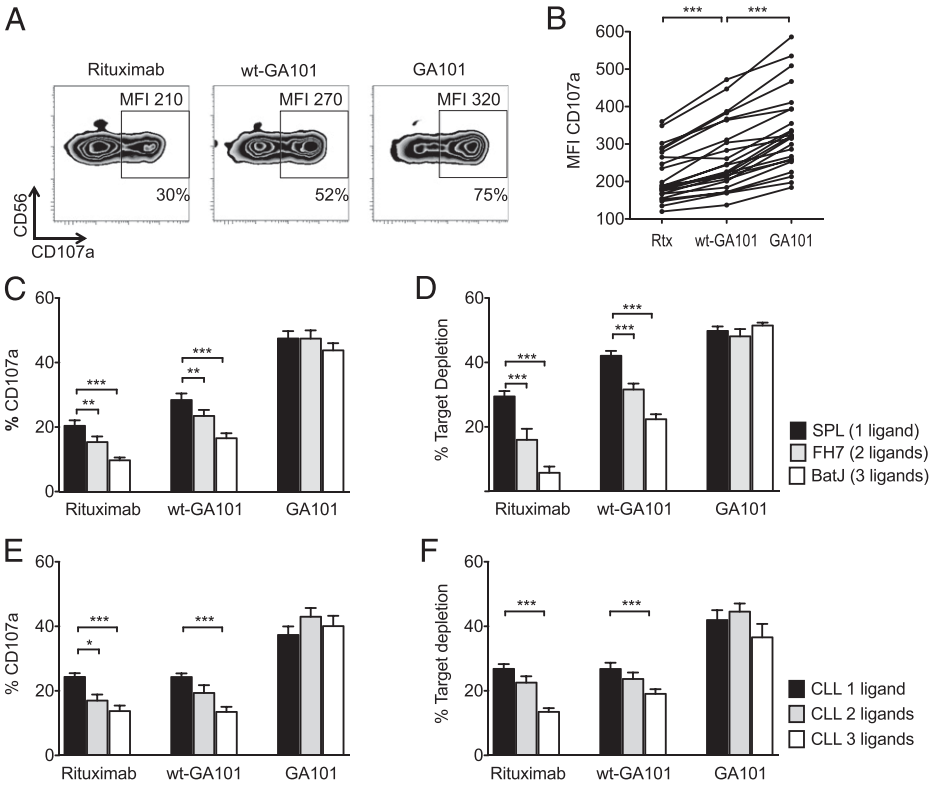

FIGURE 3. Activation and target depletion induced with GA101 are superior to nonmodified Abs. (**A**) Representative zebra plots illustrate the ability of CD20 Abs to activate NK cells. PBMCs were incubated with HLA$^-$ targets (721.221 cells) treated with rituximab, wt-GA101, and GA101 at a concentration of 0.1 μg/ml. The percentage of CD107a$^+$ cells among NK cells (CD3$^-$CD14$^-$CD19$^-$CD56$^+$) and the MFI of the CD107a$^+$ population were evaluated. (**B**) Representation of the MFI of CD107a$^+$ NK cells. The cells from 24 individuals were analyzed in a paired fashion. (**C–F**) Target cell depletion in rituximab but not GA101-driven ADCC depends on KIR/HLA interactions. Purified NK cells from individuals [n = 12/genotype (C and D); n = 11 per genotype (E and F)] lacking no, one, or two KIR ligands were incubated with target cells matched for KIR ligands either the lymphoblastoid B cell lines (SPL HLA-A*3101, B*1501, C* 0102 [C1$^+$C2$^-$Bw4$^-$]; FH7 HLA-A*0206/3002, B*3908/1801, C*0702/0501 [C1$^+$C2$^+$Bw4$^-$]; and BatJ HLA-A*0201/3101, B*4001/4402, and C*0501 [C1$^+$C2$^+$Bw4$^+$]) (C and D) or primary CLL cells (CLL with one ligand [C1$^+$C2$^-$Bw4$^-$], CLL with two ligands [C1$^-$C2$^+$Bw4$^+$ and C1$^+$C2$^-$Bw4$^+$], and CLL with three ligands [C1$^+$C2$^+$Bw4$^+$]) (E and F) previously labeled with a cell tracking dye in the presence of CD20 Abs at concentrations of 0.1 and 5 μg/ml, respectively. Bars represent the average percentage of CD107a among KIR$^+$NKG2A$^-$ NK cells (C and E) and the percentage of target cell depletion (D and F), calculated according to the following formula: 100 − (no. of dye-positive cells in the sample × 100/no. of dye positive cells in the control without Ab and effector cells). *$p \leq 0.05$, **$p \leq 0.01$, ***$p \leq 0.001$.

Target cell depletion in rituximab- but not in GA101-induced ADCC depends on KIR/HLA interactions and on frequency of unlicensed cells

To assess how levels of NK cell degranulation correspond to target cell depletion, we performed combined assays measuring both endpoints simultaneously in experiments with target cells expressing one (SPL), two (FH7), or all three (BatJ) KIR ligands. The frequency of degranulating NK cells increased proportionally to the number of missing KIR ligands with rituximab and wt-GA101, but not with GA101 (Fig. 3C). Target cell depletion showed excellent correlation with total NK cell degranulation and behaved according to the same pattern (Fig. 3D). As a result, target cell depletion induced by rituximab but not by GA101 strongly correlated with the number of KIR/HLA interactions. Similar results were obtained when healthy donor NK cells were coincubated with KIR ligand–matched primary CLL tumor cells (Fig. 3E, 3F).

Expression of KIR receptors may differ significantly between donors carrying identical KIR genes and KIR ligands (21). To assess how the KIR repertoire influences the efficacy of target cell depletion, we selected donors carrying only the HLA-C1 KIR ligand (i.e., lacking HLA-C2 and HLA-Bw4 specificities) and assessed the frequency of unlicensed (NKG2A$^-$KIR2DL3$^-$) NK cells. The frequency of these cells was then correlated to the depletion of the SPL (HLA-C2$^-$Bw4$^-$) target cells. Whereas significant correlations between the size of the unlicensed subset and target cell depletion were found for rituximab and wt-GA101, no such correlation was detected for GA101 (Fig. 4). Collectively, these data showed that, in contrast to rituximab, target cell depletion with GA101 was maximal and no longer affected by KIR/HLA interactions or by the NK cell KIR repertoire.

KIR/HLA effect synergizes with FCGR3A V158F polymorphism

To compare how the KIR ligand status compared with the FCGR3A V158F SNP in modifying NK cell activation, we typed donors for this SNP and compared activation in patients with VV, VF, or FF genotype. We found that for both rituximab and GA101, homozygous carriers of low-affinity F allele showed decreased NK cell activation after exposure to both HLA-deficient and HLA-expressing target cells, when compared with donors carrying at least one high-affinity V allele. The magnitude of the FF genotype effect was comparable to the inhibitory influence of one KIR/HLA interaction in this model and acted synergistically when present at the same time (Fig. 5).

Discussion

In this study we investigated how KIR/HLA interactions influence NK cell–mediated ADCC. Previous studies have shown that licensing, a process involving the interaction of inhibitory HLA

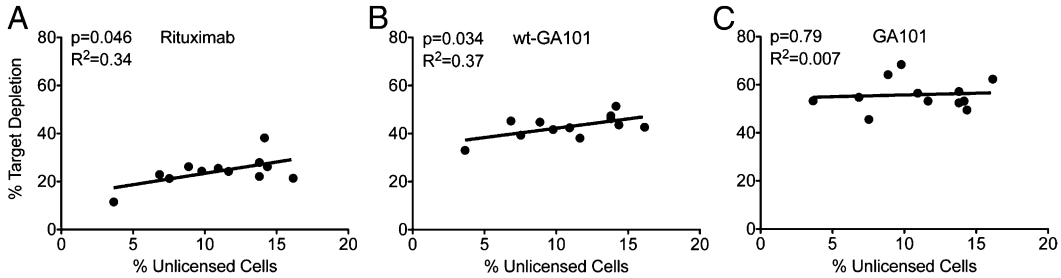

FIGURE 4. Frequency of unlicensed NK cells influences target cell depletion efficacy in ADCC induced with non-glycoengineered Abs. Purified NK cells from individuals (n = 12) lacking the HLA-C2 and Bw4 specificities were incubated with the KIR ligand–matched target B cell line (SPL [$C1^+C2^-$ $Bw4^-$]) treated with rituximab (**A**), wt-GA101 (**B**), and GA101 (**C**). All CD20 Abs were used at a concentration of 0.1 μg/ml. The percentage of $KIR2DL3^-NKG2A^-$ NK cells was correlated with target cell depletion estimated according to the following formula: 100 − (no. of dye-positive cells in the sample × 100/no. of dye-positive cells in the control without Ab and effector cells).

receptors on NK cells with HLA Ags during NK cell development, leads to augmented NK cell function, including activation via FCGR3A (13, 22). Alternatively, binding of cognate HLA KIR ligands on lymphoma cells to inhibitory KIR receptors has been shown to negatively impact rituximab-mediated ADCC (15), and Ab blockade of inhibitory KIR has recently been suggested as a way of improving rituximab efficacy (23). We were therefore interested to analyze how the opposing effects of KIR/HLA interactions affect ADCC mediated by different anti-CD20 Abs against lymphoma cells. In our analysis, we compared rituximab, the prototypic CD20 Ab, to GA101, a novel glycoengineered CD20 Ab developed to display increased capacity to elicit ADCC. The increased capacity for ADCC is the result of glycoengineering of the Fc segment of GA101. In agreement with this, preclinical studies have already shown that compared with rituximab, GA101 is more potent in inducing target cell depletion in vitro and in animal models (5, 24).

Our data confirm that licensing status affects the capacity for ADCC against HLA-deficient target B cells, with a significantly greater effect of licensing on rituximab- than on GA101-induced ADCC. When analyzing NK cell activation against target cells expressing HLA Ags, we found that KIR/HLA interactions significantly inhibited NK cell activation, resulting in unlicensed cells being the main effectors of rituximab-induced ADCC. These data suggest that of the two functionally opposing consequences of KIR/HLA interactions (increase of functional potential during NK cell maturation, decrease of function in mature NK cells encountering potential targets) the latter dominates in ADCC. Intriguingly, the inhibitory effect of KIR/HLA interactions was greatly reduced in ADCC induced by GA101. Multiple inhibitory KIR/HLA interactions were necessary to decrease GA101-induced activation of NK cells to the level achieved by rituximab (Fig. 2B). Several differences between GA101 and rituximab contribute to this difference. Glycoengineering of the Fc fragment of GA101 played an important role, as documented by the increased capacity of GA101 to activate NK cells and deplete target B cells compared with the non-glycoengineered wt-GA101 Ab. Compared to rituximab, wt-GA101 was itself more efficient in activating NK cells and depleting target B cells, indicating that increased efficacy of GA101 is not exclusively explained by differences in the Fc part, but also by the different epitope recognized, the modified elbow-hinge region, and reduced internalization of GA101 compared with rituximab (5, 24).

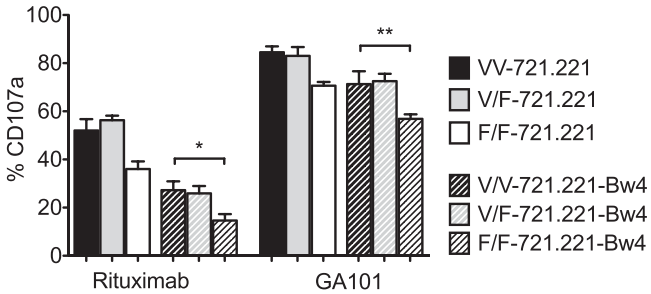

FIGURE 5. Inhibitory KIR/HLA interaction dominates over impact of FCGR3A V158F polymorphism. PBMCs from individuals expressing KIR3DL1 and its ligand HLA-Bw4 were incubated with either HLA^- (721.221) or $HLA\text{-}Bw4^+$ (721.221-Bw4) target cell lines treated with rituximab and GA101 at a concentration of 0.1 μg/ml. The level of degranulation in response to target cells and anti-CD20 Abs was compared between individuals grouped by FCGR3A genotype (high-affinity allele V, low-affinity allele F; V/V, n = 12; VF, n = 5; FF, n = 4). Bars represent the mean (±SE) percentage of $CD107a^+$ cells among $NKG2A^-$single $KIR3DL1^+$ NK cells. *$p \leq 0.05$, **$p \leq 0.01$.

The finding that rituximab-induced ADCC is primarily mediated by unlicensed NK cells is in line with similar studies performed with anti-GD2 Abs and neuroblastoma target cells (25). Interestingly, in patients with neuroblastoma, presence of KIR ligands was also shown to associate with progression-free survival after Ab treatment, with patients carrying all KIR ligands (and therefore having no KIR^+ unlicensed NK cells) responding poorly to Ab treatment (25, 26). No clinical studies have so far evaluated the role of KIR/HLA interactions in patients treated with CD20 Abs. The data presented in the present study indicate that such analyses should be performed to investigate a potential prognostic impact of KIR ligand status on response to rituximab treatment. It is intriguing to speculate that patients carrying all three KIR ligands (30–40% of whites) may particularly benefit from treatment with a novel Ab able to overcome inhibitory KIR/HLA interactions and recruit more NK cells for ADCC.

We identified the inhibitory KIR repertoire on NK cells as a second predictor of in vitro capacity for rituximab-induced ADCC, with donors carrying more unlicensed cells showing increased ADCC capacity. This is predictable given that unlicensed cells are the main effectors of rituximab-induced ADCC. Differences in KIR repertoire between donors with identical KIR genes and KIR ligands can be substantial, and previous studies have shown that in the setting of HLA haploidentity with an inhibitory KIR ligand mismatch between donor and patient, the size of the NK cell subset expressing the relevant KIR receptor predicts in vitro capacity for tumor cell killing (21). Consistent with the ability of GA101 to compensate for inhibitory KIR/HLA interactions, no association of the KIR expression repertoire with target cell depletion was detected in GA101-induced ADCC. The FCGR3A V158F polymorphism, previously identified as a predictor of clinical responses to mAb treatment, showed only a minor influence

on rituximab-induced NK cell activation in our experiments and was significantly weaker than the effect of KIR ligand status. Again, these data are in agreement with clinical data from a small cohort of neuroblastoma patients receiving treatment with an IL-2–coupled Ab, where KIR ligand status but not the FCGR3A genotype was associated with response to treatment (26).

In conclusion, our study identifies KIR/HLA interactions as strong predictors of in vitro capacity for rituximab-induced ADCC, both on the genetic (presence or absence of HLA KIR ligands) and on the KIR expression repertoire level. As a result of Fc modification leading to increased affinity to FCGR3A, the novel glycoengineered CD20 Ab GA101 is able to largely compensate for inhibitory KIR/HLA interactions. This ultimately results in the recruitment of more NK cells for ADCC, as well as increased target cell depletion being largely independent from the KIR/HLA pattern and the KIR repertoire. These in vitro data may support the recently reported increased efficacy of GA101 compared with conventional CD20 Abs in vivo (27).

Acknowledgments

We thank Andreas Buser for providing buffy coats, Karin Schmitter and Karol Czaja for preparing PBMCs, and Asensio Gonzalez and Laurent Schmied for discussion and critical reading of the manuscript.

Disclosures

C.K. is an employee of Roche Glycart.

References

1. Stern, M., and R. Herrmann. 2005. Overview of monoclonal antibodies in cancer therapy: present and promise. *Crit. Rev. Oncol. Hematol.* 54: 11–29.
2. Maloney, D. G. 2012. Anti-CD20 antibody therapy for B-cell lymphomas. *N. Engl. J. Med.* 366: 2008–2016.
3. Griffin, M. M., and N. Morley. 2013. Rituximab in the treatment of non-Hodgkin's lymphoma: a critical evaluation of randomized controlled trials. *Expert Opin. Biol. Ther.* 13: 803–811.
4. Cang, S., N. Mukhi, K. Wang, and D. Liu. 2012. Novel CD20 monoclonal antibodies for lymphoma therapy. *J. Hematol. Oncol.* 5: 64.
5. Mössner, E., P. Brünker, S. Moser, U. Püntener, C. Schmidt, S. Herter, R. Grau, C. Gerdes, A. Nopora, E. van Puijenbroek, et al. 2010. Increasing the efficacy of CD20 antibody therapy through the engineering of a new type II anti-CD20 antibody with enhanced direct and immune effector cell-mediated B-cell cytotoxicity. *Blood* 115: 4393–4402.
6. Cartron, G., L. Dacheux, G. Salles, P. Solal-Celigny, P. Bardos, P. Colombat, and H. Watier. 2002. Therapeutic activity of humanized anti-CD20 monoclonal antibody and polymorphism in IgG Fc receptor FcγRIIIa gene. *Blood* 99: 754–758.
7. Weng, W. K., and R. Levy. 2003. Two immunoglobulin G fragment C receptor polymorphisms independently predict response to rituximab in patients with follicular lymphoma. *J. Clin. Oncol.* 21: 3940–3947.
8. Mellor, J. D., M. P. Brown, H. R. Irving, J. R. Zalcberg, and A. Dobrovic. 2013. A critical review of the role of Fcγ receptor polymorphisms in the response to monoclonal antibodies in cancer. *J. Hematol. Oncol.* 6: 1.
9. Ghesquières, H., G. Cartron, J. F. Seymour, M. H. Delfau-Larue, F. Offner, P. Soubeyran, A. Perrot, P. Brice, R. Bouabdallah, A. Sonet, et al. 2012. Clinical outcome of patients with follicular lymphoma receiving chemoimmunotherapy in the PRIMA study is not affected by FCGR3A and FCGR2A polymorphisms. *Blood* 120: 2650–2657.
10. Pennell, N. M., T. Bhanji, L. Zhang, A. Seth, C. A. Sawka, and N. L. Berinstein. 2008. Lack of prognostic value of FCGR3A-V158F polymorphism in non-Hodgkin's lymphoma. *Haematologica* 93: 1265–1267.
11. Nagler, A., L. L. Lanier, S. Cwirla, and J. H. Phillips. 1989. Comparative studies of human FcRIII-positive and negative natural killer cells. *J. Immunol.* 143: 3183–3191.
12. Moretta, L., and A. Moretta. 2004. Killer immunoglobulin-like receptors. *Curr. Opin. Immunol.* 16: 626–633.
13. Anfossi, N., P. André, S. Guia, C. S. Falk, S. Roetynck, C. A. Stewart, V. Breso, C. Frassati, D. Reviron, D. Middleton, et al. 2006. Human NK cell education by inhibitory receptors for MHC class I. *Immunity* 25: 331–342.
14. Machino, T., Y. Okoshi, Y. Miyake, Y. Akatsuka, and S. Chiba. 2012. HLA-C matching status does not affect rituximab-mediated antibody-dependent cellular cytotoxicity by allogeneic natural killer cells. *Immunol. Invest.* 41: 831–846.
15. Binyamin, L., R. K. Alpaugh, T. L. Hughes, C. T. Lutz, K. S. Campbell, and L. M. Weiner. 2008. Blocking NK cell inhibitory self-recognition promotes antibody-dependent cellular cytotoxicity in a model of anti-lymphoma therapy. *J. Immunol.* 180: 6392–6401.
16. Frohn, C., P. Schlenke, B. Ebel, C. Dannenberg, G. Bein, and H. Kirchner. 1998. DNA typing for natural killer cell inhibiting HLA-Cw groups NK1 and NK2 by PCR-SSP. *J. Immunol. Methods* 218: 155–160.
17. Koehler, R. N., A. M. Walsh, N. Moqueet, J. R. Currier, M. A. Eller, L. A. Eller, F. Wabwire-Mangen, N. L. Michael, M. L. Robb, F. E. McCutchan, and G. H. Kijak. 2009. High-throughput genotyping of KIR2DL2/L3, KIR3DL1/S1, and their HLA class I ligands using real-time PCR. *Tissue Antigens* 74: 73–80.
18. Dall'Ozzo, S., C. Andres, P. Bardos, H. Watier, and G. Thibault. 2003. Rapid single-step FCGR3A genotyping based on SYBR Green I fluorescence in real-time multiplex allele-specific PCR. *J. Immunol. Methods* 277: 185–192.
19. Alter, G., J. M. Malenfant, and M. Altfeld. 2004. CD107a as a functional marker for the identification of natural killer cell activity. *J. Immunol. Methods* 294: 15–22.
20. Witzig, T. E., C. Y. Li, A. Tefferi, and J. A. Katzmann. 1994. Measurement of the intensity of cell surface antigen expression in B-cell chronic lymphocytic leukemia. *Am. J. Clin. Pathol.* 101: 312–317.
21. Pende, D., G. M. Spaggiari, S. Marcenaro, S. Martini, P. Rivera, A. Capobianco, M. Falco, E. Lanino, I. Pierri, R. Zambello, et al. 2005. Analysis of the receptor-ligand interactions in the natural killer-mediated lysis of freshly isolated myeloid or lymphoblastic leukemias: evidence for the involvement of the Poliovirus receptor (CD155) and Nectin-2 (CD112). *Blood* 105: 2066–2073.
22. Parsons, M. S., K. Zipperlen, M. Gallant, and M. Grant. 2010. Killer cell immunoglobulin-like receptor 3DL1 licenses CD16-mediated effector functions of natural killer cells. *J. Leukoc. Biol.* 88: 905–912.
23. Kohrt, H. E., A. Thielens, A. Marabelle, I. Sagiv-Barfi, C. Sola, F. Chanuc, N. Fuseri, C. Bonnafous, D. Czerwinski, A. Rajapaksa, et al. 2014. Anti-KIR antibody enhancement of anti-lymphoma activity of natural killer cells as monotherapy and in combination with anti-CD20 antibodies. *Blood* 123: 678–686.
24. Herter, S., F. Herting, O. Mundigl, I. Waldhauer, T. Weinzierl, T. Fauti, G. Muth, D. Ziegler-Landesberger, E. van Puijenbroek, S. Lang, et al. 2013. Preclinical activity of the type II CD20 antibody GA101 (obinutuzumab) compared with rituximab and ofatumumab in vitro and in xenograft models. *Mol. Cancer Ther.* 12: 2031–2042.
25. Tarek, N., J. B. Le Luduec, M. M. Gallagher, J. Zheng, J. M. Venstrom, E. Chamberlain, S. Modak, G. Heller, B. Dupont, N. K. Cheung, and K. C. Hsu. 2012. Unlicensed NK cells target neuroblastoma following anti-GD2 antibody treatment. *J. Clin. Invest.* 122: 3260–3270.
26. Delgado, D. C., J. A. Hank, J. Kolesar, D. Lorentzen, J. Gan, S. Seo, K. Kim, S. Shusterman, S. D. Gillies, R. A. Reisfeld, et al. 2010. Genotypes of NK cell KIR receptors, their ligands, and Fcγ receptors in the response of neuroblastoma patients to Hu14.18-IL2 immunotherapy. *Cancer Res.* 70: 9554–9561.
27. Goede, V., K. Fischer, R. Busch, A. Engelke, B. Eichhorst, C. M. Wendtner, T. Chagorova, J. de la Serna, M. S. Dilhuydy, T. Illmer, et al. 2014. Obinutuzumab plus chlorambucil in patients with CLL and coexisting conditions. *N. Engl. J. Med.* 370: 1101–1110.